Tsallis' *q* index and Mori's *q* phase transitions at the edge of chaos

E. Mayoral and A. Robledo

Instituto de Física, Universidad Nacional Autónoma de México, Apartado Postal 20-364, México 01000 DF, Mexico
(Received 17 January 2005; revised manuscript received 14 June 2005; published 17 August 2005)

We uncover the basis for the validity of the Tsallis statistics at the onset of chaos in logistic maps. The dynamics within the critical attractor is found to consist of an infinite family of Mori's *q*-phase transitions of rapidly decreasing strength, each associated with a discontinuity in Feigenbaum's trajectory scaling function σ. The value of *q* at each transition corresponds to the same special value for the entropic index *q*, such that the resultant sets of *q*-Lyapunov coefficients are equal to the Tsallis rates of entropy evolution.

I. INTRODUCTION

Searches for evidence of nonextensive [1,2] properties at the period-doubling onset of chaos in logistic maps—the Feigenbaum attractor—have at all times yielded affirmative responses, from the initial numerical studies [3] to subsequent heuristic investigations [4], and the more recent rigorous results [5,6]. However, a critical analysis and a genuine understanding of the basis for the validity at this attractor of the nonextensive generalization [1,2] of the Boltzmann–Gibbs (BG) statistical mechanics—here referred to as *q*-statistics—is until now lacking. In this paper, we clarify the circumstances under which the features of *q*-statistics are observed and, most importantly, we demonstrate that the mechanism by means of which the Tsallis entropic index *q* arises is provided by the occurrence of dynamical phase transitions of the kind described by the formalism of Mori and colleagues [7]. These transitions, similar to first-order thermal phase transitions, are associated with trajectories that link different regions within a multifractal attractor. The onset of chaos is an incipiently chaotic attractor, with memory-preserving, nonmixing, phase-space trajectories. Because many of its properties are familiar, and have been well understood for many years, it is of interest to explain how previous knowledge fits in with this different perspective.

The Feigenbaum attractor is the classic one-dimensional critical attractor with universal properties in the renormalization group (RG) sense, i.e., shared by all unimodal (one hump) maps with the same degree of nonlinearity. The static or geometrical properties of this attractor have been understood since long ago [8–10] and are represented, for example, by the generalized dimensions $D(\mathsf{q})$ or the spectrum of dimensions $f(\widetilde{\alpha})$ that characterize the multifractal set [9,10]. The dynamical properties that involve positions within the attractor also display universality, and, as we see below, these are conveniently given in terms of the discontinuities in Feigenbaum's trajectory scaling function σ, which measures the convergence of positions in the orbits of period 2^n as $n \to \infty$ [8]. Let us first recall that the Feigenbaum attractor has a vanishing ordinary Lyapunov coefficient λ_1 and that the sensitivity to initial conditions ξ_t does not converge to any single-valued function and displays fluctuations that grow indefinitely [7,12–14]. For initial positions at the attractor ξ_t develops a universal self-similar temporal structure

and its envelope grows with *t* as a power law [3,7,12–14]. We are interested here in determining the detailed dependence of the aforementioned structure on *both* the initial position x_0 and the observation time *t* as this dependence is preserved by the infinitely lasting memory. Therefore, we shall not consider the effect of averaging with respect to x_0 and/or *t*, explored in other studies [12,15], as this would obscure the fine points of the dynamics.

The central assertion of the *q* statistics with regard to the dynamics of critical attractors is a sensitivity to initial conditions ξ_t associated to the *q*-exponential functional form, i.e., the "*q*-deformed" exponential function $\exp_q(x) \equiv [1-(q-1)x]^{-1/(q-1)}$. From such ξ_t a *q*-generalized Lyapunov coefficient λ_q can be determined just as λ_1 is read from an exponential ξ_t. The λ_q is presumed to satisfy a *q*-generalized identity $\lambda_q = K_q$ [10,16] where K_q is an entropy production rate based on the Tsallis entropy S_q, defined in terms of the *q*-logarithmic function $\ln_q y \equiv (y^{1-q}-1)/(1-q)$, the inverse of $\exp_q(x)$. Unlike λ_1 for (ergodic) chaotic attractors, the coefficient λ_q is dependent on the initial position x_0 and therefore λ_q constitutes a spectrum (and also K_q) that can be examined by varying this position.

The *fixed* values of the entropic index *q* are obtained from the universality class parameters to which the attractor belongs. For the simpler pitchfork and tangent bifurcations there is a single well-defined value for the index *q* for each type of attractor as a single *q*-exponential describes the sensitivity [19]. For multifractal critical attractors, the situation is more complicated and there appears to be a multiplicity of indexes *q* but with precise values given by the attractor scaling functions. As shown below, the sensitivity takes the form of a family of interweaved *q* exponentials. The *q* indexes appear in conjugate pairs, *q* and $Q = 2 - q$, as these correspond to switching the starting and finishing trajectory positions. We show that *q* and *Q* are related to the occurrence of pairs of dynamical "*q*-phase" transitions, which connect qualitatively different regions of the attractor [7,14]. These transitions are identified as the source of the special values for the entropic index *q*. For the Feigenbaum attractor an infinite family of such transitions take place but are of rapidly decreasing strength.

In Sec. II we recall the essential features of the statistical-mechanical formalism of Mori and colleagues [7] to study dynamical phase transitions in attractors of nonlinear maps

and follow this by a summary of expressions of the q statistics. Then, in subsequent sections we present known properties and develop others for the dynamics within the Feigenbaum attractor. Among these we derive the sensitivity ξ_t, in terms of the trajectory scaling function σ, and use this to make contact with both Mori's and Tsallis' schemes. We discuss our results.

II. STATISTICAL MECHANICS FOR CRITICAL ATTRACTORS

During the late 1980s Mori and coworkers developed a comprehensive thermodynamic formalism to characterize drastic changes at bifurcations and at other singular phenomena in low dimensional maps [7]. The formalism was further adapted to study critical attractors and was illustrated by considering the specific case of the period-doubling onset of chaos in the logistic map [7,13,14]. For critical attactors the scheme involves the evaluation of fluctuations of the generalized finite-time Lyapunov coefficient

$$\lambda(t,x_0) = \frac{1}{\ln t}\sum_{i=0}^{t-1} \ln \left| \frac{df_{\mu_\infty}(x_i)}{dx_i} \right|, \quad t \gg 1, \tag{1}$$

where $f_\mu(x)$ is here the logistic map, or its extension to non-linearity of order $z > 1$,

$$f_\mu(x) = 1 - \mu|x|^z, \quad -1 \le x \le 1, \quad 0 \le \mu \le 2. \tag{2}$$

We denote by $\mu_\infty(z)$ the value of the control parameter μ at the onset of chaos, with $\mu_\infty(2) = 1.40115\ldots$. Note the replacement of the customary t by $\ln t$ in Eq. (1), as the ordinary Lyapunov coefficient λ_1 vanishes for critical attractors, here at μ_∞, $t \to \infty$.

The density distribution for the values of λ, at $t \gg 1$, $P(\lambda,t)$, is written in the form [7,14]

$$P(\lambda,t) = t^{-\psi(\lambda)}P(0,t), \tag{3}$$

where $\psi(\lambda)$ is a concave spectrum of the fluctuations of λ with minimum $\psi(0)=0$ and is obtained as the Legendre transform of the "free energy" function $\phi(\mathsf{q})$, defined as

$$\phi(\mathsf{q}) \equiv -\lim_{t\to\infty} \frac{\ln Z(t,\mathsf{q})}{\ln t}, \tag{4}$$

where $Z(t,\mathsf{q})$ is the dynamic partition function

$$Z(t,\mathsf{q}) \equiv \int d\lambda P(\lambda,t) t^{-(\mathsf{q}-1)\lambda}. \tag{5}$$

The "coarse-grained" function of generalized Lyapunov coefficients $\lambda(\mathsf{q})$ and the variance $v(\mathsf{q})$ of $P(\lambda,t)$ are given, respectively, by [7,14]

$$\lambda(\mathsf{q}) \equiv \frac{d\phi(\mathsf{q})}{d\mathsf{q}} \quad \text{and} \quad v(\mathsf{q}) \equiv \frac{d\lambda(\mathsf{q})}{d\mathsf{q}}. \tag{6}$$

Note the special weight $t^{-(\mathsf{q}-1)\lambda}$ in $Z(t,\mathsf{q})$ and in the quantities derived from it. The functions $\phi(\mathsf{q})$ and $\psi(\lambda)$ are the dynamic counterparts of the Renyi dimensions $D(\mathsf{q})$ and the spectrum $f(\tilde{\alpha})$ that characterize the geometric structure of the attractor [9].

As with ordinary thermal first-order phase transitions, a q-phase transition is indicated by a section of linear slope $m_c = 1 - q$ in the spectrum (free energy) $\psi(\lambda)$, a discontinuity at $\mathsf{q}=q$ in the Lyapunov function (order parameter) $\lambda(\mathsf{q})$, and a divergence at q in the variance (susceptibility) $v(\mathsf{q})$. For the onset of chaos at $\mu_\infty(z=2)$, a single q-phase transition was numerically determined [7–13] and found to occur at a value close to $m_c = -(1-q) \simeq -0.7$. Arguments were provided [7–13] for this value to be $m_c = -(1-q) = -\ln 2/\ln \alpha = -0.7555\ldots$, where $\alpha = 2.50290\ldots$ is one of the Feigenbaum's universal constants. Our analysis below shows that this initial result gives a broad picture of the dynamics at the Feigenbaum attractor and that actually an infinite family of q-phase transitions of decreasing magnitude takes place at μ_∞.

Independently, Tsallis *et al.* [3] proposed that for critical attractors, the sensitivity to initial conditions ξ_t [defined as $\xi_t(x_0) \equiv \lim_{\Delta x_0 \to 0} (\Delta x_t/\Delta x_0)$ where Δx_0 is the initial separation of two orbits and Δx_t that at time t] has the form

$$\xi_t(x_0) = \exp_q[\lambda_q(x_0)t], \tag{7}$$

which yields the customary exponential ξ_t with λ_1 when $q \to 1$. In Eq. (7) q is the entropic index and the initial-position-dependent $\lambda_q(x_0)$ are the q-generalized Lyapunov coefficients. Tsallis *et al.* [3] also suggested that the identity $K_1 = \lambda_1$ [16], where the rate of entropy production K_1 is given by

$$K_1 t = S_1(t) - S_1(0), \quad t \text{ large}, \tag{8}$$

and

$$S_1 = -\sum_i p_i \ln p_i, \tag{9}$$

for an ensemble of trajectories with instantaneous distribution p_i, would be generalized to $K_q = \lambda_q$, where the q-generalized rate of entropy production K_q is defined via

$$K_q t = S_q(t) - S_q(0), \quad t \text{ large}, \tag{10}$$

and where

$$S_q \equiv \sum_i p_i \ln_q p_i^{-1} = \frac{1 - \sum_i^W p_i^q}{q - 1} \tag{11}$$

is the Tsallis entropy. These properties have been corroborated to hold at $\mu_\infty(z)$ numerically [3,15] for sets of trajectories with x_0 spread throughout $-1 \le x_0 \le 1$ and analytically for specific classes of trajectories starting near $x_0 = 0$ and observed at specific times of the form $t = (2k+1)2^n - 1$, $k = 0,1,2\ldots$, and $n = 1,2,\ldots$ [5–17]. We explain the rationale for these particular choices of x_0 and t in Sec. III where we examine the structure of trajectories inside the attractor (see Fig. 1).

III. DYNAMICS WITHIN THE FEIGENBAUM ATTRACTOR

In Fig. 1(a) we have plotted (in logarithmic scales), the first few absolute values of iterated positions $|x_t|$ of the orbit
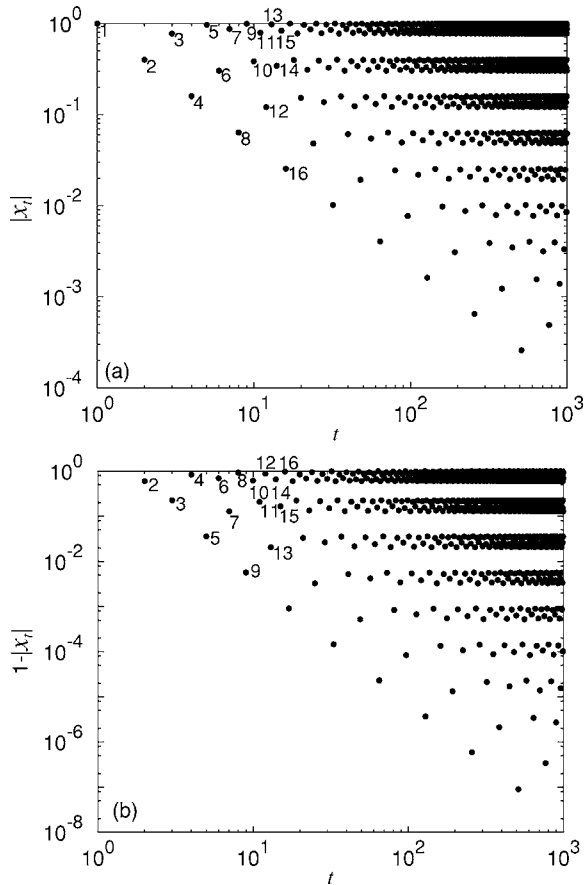
FIG. 1. (a) Absolute values of $|x_t|$ vs t in logarithmic scales for the orbit with initial condition $x_0=0$ at μ_∞ of the logistic map $z=2$. The labels indicate iteration time t. (b) Same as (a) with $|x_t|$ replaced by $1-|x_t|$.

at $\mu_\infty(z=2)$ starting at $x_0=0$ where the labels indicate iteration time t. Note the structure of horizontal bands and that in the top band lie half of the attractor positions (odd times), in the second band a quarter of the attractor positions, and so on. The top band is eliminated by functional composition of the original map, that is by considering the orbit generated by the map $f_{\mu_\infty}^{(2)}(0)$ instead of $f_{\mu_\infty}(0)$. Successive bands are eliminated by considering the orbits of $f_{\mu_\infty}^{(2^j)}(0)$, $j=1,2\ldots$. The positions of the top band (odd times) can be reproduced approximately by the positions of the band below it (times of the form $t=2+4n$, $n=0,1,2\ldots$) by multiplication by a factor equal to α, e.g., $|x_1|\simeq\alpha|x_2|$. Likewise, the positions of the second band are reproduced by the positions of the third band under multiplication by α, e.g., $|x_2|\simeq\alpha|x_4|$, and so on. In Fig. 1(b) we show a logarithmic scale plot of $1-|x_t|$ that displays a band structure similar to that in Fig. 1(a), in the top band lie again half of the attractor positions (even times) and below the other half (odd times) is distributed in the subsequent bands. This time the positions in one band are reproduced approximately from the positions of the band lying below it by multiplication by a factor α^z, e.g., $1-|x_3|\simeq\alpha^z(1-|x_5|)$. The properties among bands of iterate positions merely follow from repeated composition and rescaling of the map and represent a graphical construction of the

Feigenbaum RG transformation $Rf(x)\equiv\alpha f(f(x/\alpha))$, where $\alpha(z=2)=2.50290\ldots$.

Also, the trajectory with initial condition $x_0=0$ maps out the Feigenbaum attractor in such a way that the absolute values of succeeding (time-shifted $\tau=t+1$) positions $|x_\tau|$ form subsequences with a common power-law decay of the form $\tau^{-1/1-q}$ with $q=1-\ln 2/\ln\alpha(z)$, with $q\simeq0.24449$ when $z=2$. See how positions fall along straight diagonal lines in Fig. 1(a). That is, the *entire* attractor can be decomposed into position subsequences generated by the time subsequences $\tau=(2k+1)2^n$, each obtained by running over $n=0,1,2,\ldots$ for a fixed value of $k=0,1,2,\ldots$. Noticeably, the positions in these subsequences can be obtained from those belonging to the "superstable" periodic orbits of lengths 2^n, i.e., the 2^n-cycles that contain the point $x=0$ at $\bar\mu_n<\mu_c(0)$ [8]. Specifically, the positions for the main subsequence $k=0$, that constitutes the lower bound of the entire trajectory [see Fig. 1(a)], can be identified to be $|x_{2^n}|\simeq d_{n,0}=\alpha^{-n}$, where $d_{n,0}\equiv|f_{\bar\mu_n}^{(2^{n-1})}(0)|$ is the "nth principal diameter" defined at the 2^n-supercycle, the distance of the orbit position nearest to $x=0$ [8]. The main subsequence can be expressed as

$$|x_t|=\exp_{2-q}(-\Lambda_q t) \tag{12}$$

with $\Lambda_q=(z-1)\ln\alpha/\ln 2$. Interestingly, this analytical result for $|x_t|$ can be seen to satisfy the dynamical fixed-point relation, $h(t)=\alpha h[h(t/\alpha)]$ with $\alpha=2^{1/(1-q)}$. See [5,6] for $z=2$ and [17] for general $z>1$.

We now work out the relationship between the trajectory scaling function σ and the sensitivity ξ_t at μ_∞. To begin with we recall [8] the general definition of the diameters $d_{n,m}$ that measure the bifurcation forks that form the period-doubling cascade sequence. The $d_{n,m}$ in these orbits are defined as the distances of the elements x_m, $m=0,1,2,\ldots,2^n-1$, to their nearest neighbors $f_{\bar\mu_n}^{(2^{n-1})}(x_m)$, i.e.,

$$d_{n,m}\equiv f_{\bar\mu_n}^{(m+2^{n-1})}(0)-f_{\bar\mu_n}^{(m)}(0). \tag{13}$$

For large n, $d_{n,0}/d_{n+1,0}\simeq-\alpha(z)$; $\alpha(2)=\alpha$. Furthermore, Feigenbaum [11] constructed the auxiliary function

$$\sigma_n(m)=\frac{d_{n+1,m}}{d_{n,m}} \tag{14}$$

to quantify the rate of change of the diameters and showed that in the limit $n\to\infty$ it has finite (jump) discontinuities at all rationals of the form $m/2^{n+1}$. So, considering the variable $y=m/2^{n+1}$ one obtains [8,11], omitting the subindex n, $\sigma(0)=-1/\alpha$, but $\sigma(0^+)=1/\alpha^z$, and through the antiperiodic property $\sigma(y+1/2)=-\sigma(y)$, also $\sigma(1/2)=1/\alpha$, but $\sigma(1/2+0^+)=-1/\alpha^z$. Other discontinuities in $\sigma(y)$ appear at $y=1/4,1/8,3/8$, etc. In most cases it is only necessary to consider the first few as their magnitude decreases rapidly (see, e.g., Fig. 31 in Ref. [8]). The discontinuities of $\sigma_n(m)$ can be suitably obtained by first generating the superstable orbit 2^∞ at μ_∞ and then plotting the position differences $|x_t-x_m|=|f_{\mu_\infty}^{(t)}(0)-f_{\mu_\infty}^{(m)}(0)|$ for times of the form $t=2^n-m$, $n=0,1,2,\ldots$, in logarithmic scales. The distances that separate positions along the time subsequence correspond to the loga-

rithm of the diameters $d_{n,m}$. See Figs. 1(a) and 1(b) where the constant spacing of positions along the main diagonal provide the values for $\ln d_{n,0} \simeq -n \ln \alpha$ and $\ln d_{n,1} \simeq -n \ln \alpha^z$, respectively. The constant slope s_m of the resulting time subsequence data is related to $\sigma_n(m)$, i.e., $\sigma_n(m) = 2^{s_m}$. See Figs. 1(a) and 1(b) where the slopes of the main diagonal subsequences have the values $-\ln \alpha / \ln 2$ and $-z \ln \alpha / \ln 2$, respectively. From these two slopes the value of the largest jump discontinuity of $\sigma_n(m)$ is conveniently determined.

A key factor in obtaining our results is the fact that the sensitivity $\xi_t(x_0)$ can be evaluated for trajectories within the attractor via consideration of the discontinuities of $\sigma(y)$. Our strategy for determining $\xi_t(x_0)$ is to chose the initial and the final separation of the trajectories to be the diameters $\Delta x_0 = d_{n,m}$ and $\Delta x_t = d_{n,m+t}$, $t = 2^n - 1$, respectively. Then, $\xi_t(x_0)$ is obtained as

$$\xi_t(x_0) = \lim_{n \to \infty} \left| \frac{d_{n,m+t}}{d_{n,m}} \right|^n. \tag{15}$$

Note that in this limit $\Delta x_0 \to 0$, $t \to \infty$ *and* the 2^n-supercycle becomes the onset of chaos (the 2^∞-supercycle). Then, $\xi_t(x_0)$ can be written as

$$\xi_t(m) \simeq \left| \frac{\sigma_n(m-1)}{\sigma_n(m)} \right|^n, \quad t = 2^n - 1, \quad n \text{ large}, \tag{16}$$

where we have used $|\sigma_n(m)|^n \simeq \Pi_{i=1}^n |d_{i+1,m}/d_{i,m}|$ and $d_{i+1,m+2^n} = -d_{i+1,m}$. Note that for the inverse process, starting at $\Delta x_0 = d_{n,m+t} = -d_{n,m-1}$ and ending at $\Delta x_{t'} = d_{n,m} = -d_{n,m-1+t'}$, with $t' = 2^n + 1$ one obtains

$$\xi_{t'}(m-1) \simeq \left| \frac{\sigma_n(m)}{\sigma_n(m-1)} \right|^n, \quad t' = 2^n + 1, \quad n \text{ large}. \tag{17}$$

Given the known properties of $\sigma_n(m)$ we can readily extract those for $\xi_t(m)$ for general nonlinearity $z > 1$. Taking into account only the first $2M$, $M = 1, 2, \ldots$ discontinuities of $\sigma_n(m)$ we have the antiperiodic step function

$$1/\sigma_n(m) = \begin{cases} \alpha_l, & l2^{n-M} \leq m < (l+1)2^{n-M} \\ -\alpha_l, & (2^M+l)2^{n-M} \leq m < (2^M+l+1)2^{n-M}, \end{cases} \tag{18}$$

with $l = 0, 1, \ldots, 2^M - 1$, and this implies that $\xi_t(m) = 1$ when $\sigma_n(m)$ is continuous at m, and

$$\xi_t(m) = \left| \frac{\alpha_l}{\alpha_{l+1}} \right|^n, \quad \text{or}, \quad \xi_{t'}(m) = \left| \frac{\alpha_l}{\alpha_{l+1}} \right|^{-n}, \tag{19}$$

when $\sigma_n(m)$ has a discontinuity at $m = l2^{n-M}$. As we make clear below, these behaviors for the sensitivity reflect the multiregion nature of the multifractal attractor and the memory retention of these regions in the dynamics. Thus, $\xi_t(m) = 1$ (or $\lambda_q(x_0) = 0$) corresponds to trajectories that depart and arrive in the same region, while the power laws in Eq. (19) correspond to a departing position in one region and arrival at a different region and vice versa, the trajectories expand in one sense and contract in the other.

IV. ORIGIN OF TSALLIS' q INDEX

We now make explicit the mentioned link between the occurrence of Mori's q-phase transitions and the q-statistical dynamical properties at μ_∞. Consider $M = 1$, the simplest approximation to $\sigma_n(m)$, yet it captures the effect on ξ_t of the most dominant trajectories within the attractor. This is to assume that half of the diameters scales as $\alpha_0 = \alpha^z$ (as in the most crowded region of the attractor, $x \simeq 1$) while the other half scales as $\alpha_1 = \alpha$ (as in the most sparse region of the attractor, $x \simeq 0$). With use of the identity $A^n = [1 + t/(2k+1)]^{\ln A/\ln 2}$, $t = 2^n - (2k+1)$, $\xi_t(m) = |\alpha_0/\alpha_1|^n$ can be rewritten as the q-exponential

$$\xi_t(m) = \exp_{q_0}[\lambda_{q_0}^{(k)} t], \tag{20}$$

where

$$q_0 = 1 - \frac{\ln 2}{(z-1)\ln \alpha}, \tag{21}$$

and where

$$\lambda_{q_0}^{(k)} = \frac{(z-1)\ln \alpha}{(2k+1)\ln 2}, \quad k = 0, 1, \ldots . \tag{22}$$

The $(2k+1)^{-1}$ term in $\lambda_{q_0}^{(k)}$ arises from the time shift involved in selecting different initial positions $x_0 \simeq 1$ (see Fig. 1 and Ref. [6]). Similarly, the sensitivity for the trajectories in the inverse order yields

$$\xi_{t'}(m) = \exp_{Q_0}[\lambda_{Q_0}^{(k)} t], \tag{23}$$

where $Q_0 = 2 - q_0$, and where $\lambda_{Q_0}^{(k)} = -2\lambda_{q_0}^{(k)}$. The factor of 2 in $\lambda_{Q_0}^{(k)}$ appears because of a basic difference between the orbits of periods 2^n and 2^∞. In the latter case, to reach $x_{t'} \simeq 0$ from $x_0 \simeq 1$ at times $t' = 2^n + 1$ the iterate necessarily moves into positions of the next period 2^{n+1}, and orbit contraction is twice as effective than expansion. Note that the relationship between the indexes $Q_0 = 2 - q_0$ for the couple of conjugate trajectories stems from the property $\exp_q(x) = 1/\exp_{2-q}(-x)$. For $z = 2$ one obtains $Q_0 \simeq 1.7555$ and $q_0 \simeq 0.2445$, this latter value agrees with that obtained in several earlier studies [3,6]. From the results for $\lambda_{q_0}^{(k)}$ and $\lambda_{Q_0}^{(k)}$ we can construct the two-step Lyapunov function

$$\lambda(\mathsf{q}) = \begin{cases} \lambda_{q_0}^{(0)}, & -\infty < \mathsf{q} \leq q_0, \\ 0, & q_0 < \mathsf{q} < Q_0, \\ \lambda_{Q_0}^{(0)}, & Q_0 \leq \mathsf{q} < \infty. \end{cases} \tag{24}$$

For $z = 2$ one has $\lambda_{q_0}^{(0)} = \ln \alpha / \ln 2 \simeq 1.323$ and $\lambda_{Q_0}^{(0)} = -2\lambda_{q_0}^{(0)} \simeq -2.646$ [see Fig. 2(a)].

When the next discontinuities of importance in $\sigma(y)$ are taken into account new information on $\xi_t(x_0)$ is obtained in the form of additional pairs of q-exponentials as in Eqs. (20) and (23). In the next approximation for $\sigma_n(m)$ there are four scaling factors, $\alpha_0 = \alpha^z$, α_1, α_2, $\alpha_3 = \alpha$, where $\alpha_1 = 1/\sigma(1/4)$ (with $\alpha_1 \simeq 5.458$ for $z = 2$) and $\alpha_2 = 1/\sigma(3/4)$ (with $\alpha_2 \simeq 2.195$ for $z = 2$). These last values are associated to the two "midway" regions between the most crowded and most
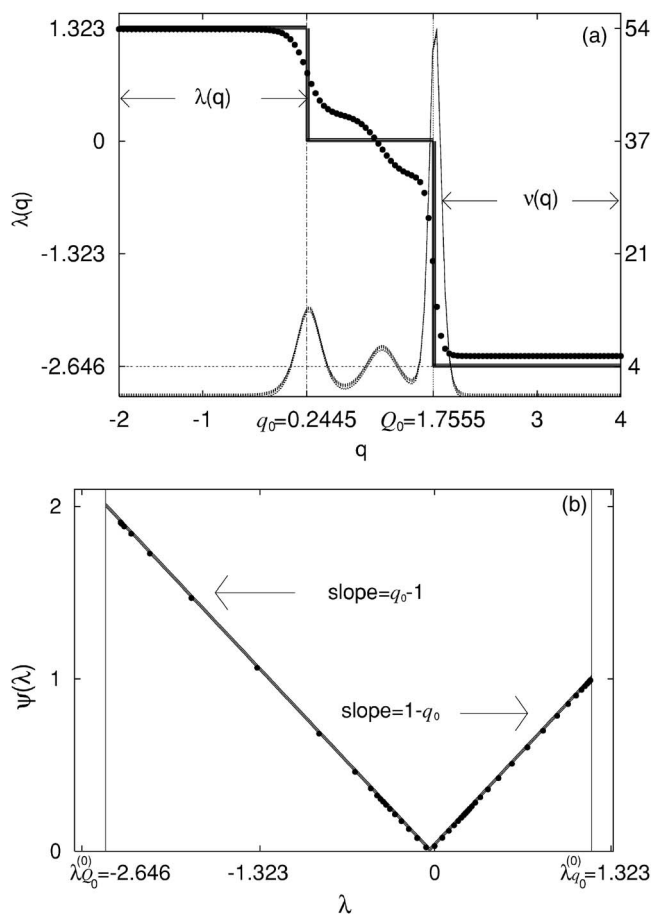
FIG. 2. q-phase transitions for the main discontinuity in $\sigma_n(m)$ with index values q_0 and $Q_0 = 2 - q_0$. The solid lines are the piecewise continuous functions given in the text, whereas the solid circles are the same functions calculated from the partition function $Z(t, q)$ with the piecewise $\psi(\lambda)$ as input. See text for details.

sparse regions of the attractor. We have now three values for the q index, q_0, q_1, and q_2 (together with the conjugate values $Q_0 = 2 - q_0$, $Q_1 = 2 - q_1$ and $Q_2 = 2 - q_2$ for the inverse trajectories). For each value of q there is a set of q-Lyapunov coefficients running from a maximum $\lambda_{q_j,\max}$ to zero (or a minimum $\lambda_{Q_j,\min}$ to zero). From the results for $\lambda_{q_j}^{(k)}$ and $\lambda_{Q_j}^{(k)}$, $j = 0, 1, 2$ we can construct three Lyapunov functions $\lambda_j(q)$, $-\infty < q < \infty$, each with two jumps located at $q = q_j = 1 - \ln 2 / \ln \alpha_j(z)/\alpha(z)$ and $q = Q_j = 2 - q_j$. Similar results are obtained when more discontinuities in $\sigma_n(m)$ are taken into account.

Direct contact can be established now with the formalism developed by Mori and coworkers and the q-phase transition reported in Ref. [14]. Each step function for $\lambda(q)$ can be integrated to obtain the spectrum $\phi(q)$ ($\lambda(q) \equiv d\phi/dq$) and from this its Legendre transform $\psi(\lambda)[\equiv \phi - (1 - q)\lambda]$. We illustrate this with the $\sigma_n(m)$ approximated with only two scale factors and present specific values when $z = 2$. The free energy functions $\phi(q)$ and $\psi(\lambda)$ obtained from the two-step $\lambda(q)$ determined above and shown in Fig. 2(a) are given by

$$\phi(q) = \begin{cases} \lambda_{q_0}^{(0)}(q - q_0), & q \leq q_0, \\ 0, & q_0 < q < Q_0, \\ \lambda_{Q_0}^{(0)}(q - Q_0), & q \geq Q_0, \end{cases} \tag{25}$$

and

$$\psi(\lambda) = \begin{cases} (1 - Q_0)\lambda, & \lambda_{Q_0}^{(0)} < \lambda < 0, \\ (1 - q_0)\lambda, & 0 < \lambda < \lambda_{q_0}^{(0)}. \end{cases} \tag{26}$$

See Fig. 2(b). The constant slopes of $\psi(\lambda)$ represent the q-phase transitions associated to trajectories linking two regions of the attractor, $x \simeq 1$ and $x \simeq 0$, and their values $1 - q_0$ and $q_0 - 1$ correspond the index q_0 obtained for the q-exponentials ξ_t in Eqs. (20) and (23). The slope $q_0 - 1 \simeq -0.7555$ coincides with that originally detected in Refs. [13,14]. When we consider also the next discontinuities of importance in $\sigma(y)$ at $y = 1/4, 3/4$ we obtain a couple of two q-phase transitions for each of the three values of the q index, q_0, q_1, and q_2. The constant slope values for the q-phase transitions at $1 - q_0$ and $q_0 - 1$ appear again, but now we have two other pairs of transitions with slope values $1 - q_1$ and $q_1 - 1$, and, $1 - q_2$ and $q_2 - 1$, that correspond, respectively, to orbits that link the most crowded region of the attractor to the "medium crowded" region, and to orbits that link this medium crowded region with the "medium sparse" region of the attractor.

V. EQUALITY BETWEEN q-LYAPUNOV COEFFICIENTS AND RATE OF q-ENTROPY CHANGE

Next, we verify the equality between the q-Lyapunov coefficients $\lambda_{qi}^{(k)}$ and the q-generalized rates of entropy production $K_{q_i}^{(k)}$. We follow the same procedure as in Ref. [6]. Consider a large number $\mathcal{N}$ of trajectories with initial positions uniformly distributed within a small interval of length Δx_0 containing the attractor point x_0. A partition of this interval is made with N nonintersecting intervals of lengths $\varepsilon_{i,0}$ ($i = 1, 2, \ldots, N$). For Δx_0 sufficiently small, after $t = 2^n - 1$, or $t' = 2^n + 1$, iterations these interval lengths transform according to

$$\frac{\varepsilon_{i,t}}{\varepsilon_{i,0}} = \left| \frac{\alpha_l}{\alpha_{l+1}} \right|^n \quad \text{or} \quad \frac{\varepsilon_{i,t'}}{\varepsilon_{i,0}} = \left| \frac{\alpha_l}{\alpha_{l+1}} \right|^{-n} \tag{27}$$

(recall $\sigma_n(m)$ has a discontinuity at $m = l2^{n-M}$). We observe that the interval ratios remain constant; that is, $\varepsilon_{i,0}/\Delta x_0 = \varepsilon_{i,t}/\Delta x_t$, since the entire-interval ratio $\Delta x_t/\Delta x_0$ scales equally with t. Thus, the initial number of trajectories within each interval $\mathcal{N}\varepsilon_{i,0}/\Delta x_0$ remains fixed in time, with the consequence that the original distribution stays *uniform* for all times $t < T$, where $T \to \infty$ as $\Delta x_0 \to 0$. We can now calculate the rate of entropy production. This is more easily done with the use of a partition of W equal-sized cells of length ε. If we denote by W_t the number of cells that the ensemble occupies at time t and by Δx_t the total length of the interval these cells form, we have $W_t = \Delta x_t/\varepsilon$ or $W_t = (\Delta x_t/\Delta x_0)(\Delta x_0/\varepsilon)$, and in the limit $\varepsilon \to 0$, $\Delta x_0/\varepsilon \to 1$ we obtain the simple result $W_t = \xi_t$. As the distribution is uniform, and recalling that Eq. (7)

for ξ_t holds in all cases, the q entropy is given by

$$S_{q_j}(t) = \ln_{q_j} W_t = \lambda_{q_j}^{(k)} t, \qquad (28)$$

while $K_{q_j}^{(k)} = \lambda_{q_j}^{(k)}$, as $W_{t=0} = 1$.

It is important to clarify the circumstances under which the equalities $\lambda_q^{(k)} = K_q^{(k)}$ are obtained as these could be interpreted as shortcomings of the formalism. First of all, the rate K_q does not generalize the trajectory-based Kolmogorov–Sinai (KS) entropy $\mathcal{K}_1$ that is involved in the well-known Pesin identity $\lambda_1 = \mathcal{K}_1$ [8–10]. Presumably, the q-generalized KS entropy $\mathcal{K}_q$ would be defined in the same manner as $\mathcal{K}_1$ with the use of S_q in place of S_1. The rate K_q is determined from values of S_q only at two different times [10]. The relationship between $\mathcal{K}_1$ and K_1 has been investigated for several chaotic maps [18], and it has been established that the equality $\mathcal{K}_1 = K_1$ occurs during an intermediate stage in the evolution of the entropy $S_1(t)$, after an initial transient dependent on the initial distribution of positions and before an asymptotic approach to a constant saturation value. Here we have seemingly looked into the analogous intermediate regime in which one would expect $\mathcal{K}_q = K_q$, as we explain below, however, the answer to this question is not analyzed in this paper.

We have only considered initial conditions within small distances outside the positions of the Feigenbaum attractor and have not focused on the initial transient behavior referred to in the above paragraph. As for the final asymptotic regime mentioned above, it should be kept in mind that the distance between trajectories, from which we obtain λ_q, always saturates because of the finiteness of the available phase space (the multifractal subset of $[-1,1]$ that is the Feigenbaum attractor). It is widely known [10] that special care needs to be taken in determining λ_1 from a time series to avoid saturation due to folding and similar limitations occur for $\lambda_q^{(k)}$. Separation of incipiently chaotic trajectories, just as separation of chaotic ones, undergo two different processes: stretching, which leads to the q-exponential regime in ξ_t, and folding, which keeps the orbits bounded. Therefore for t, sufficiently large Eq. (7) would be no longer valid, just as in the exponential ξ_t of chaotic attractors. This is the reason there is a saturation time T in our determination of $\lambda_q^{(k)}$, and this, consequently, supports our use of the rates $K_q^{(k)}$ in $\lambda_q^{(k)} = K_q^{(k)}$.

VI. CONCLUDING REMARKS

Our most striking finding is that the dynamics at the onset of chaos is constituted by an infinite family of Mori's q-phase transitions, each associated to orbits that have common starting and finishing positions located at specific regions of the attractor. Each of these transitions is related to a discontinuity in the σ function of "diameter ratios," and this, in turn, implies a q exponential ξ_t and a spectrum of q-Lyapunov coefficients—equal to the Tsallis rate of entropy production—for each set of attractor regions. The transitions come in pairs with specific conjugate indexes q and $Q = 2 - q$, as these correspond to switching the starting and finishing orbital positions. Since the amplitude of the discontinui-

ties in σ diminishes rapidly, in practical terms there is only need of evaluation for the first few of them. The dominant discontinuity is associated to the most crowded and sparse regions of the attractor, and this alone provides a very reasonable description of the dynamics, as found in earlier studies [3–6]. The special values for the Tsallis entropic index q in ξ_t are equal to the special values of the variable q in the formalism of Mori and colleagues at which the q-phase transitions take place. Therefore, we have identified the cause or source for the entropic index q observed at the Feigenbaum attractor.

We found that the sensitivity to initial conditions at the onset of chaos does not have the form of a single q exponential but of infinitely many interlaced q exponentials. More precisely, we found a hierarchy of such families of interlaced q exponentials. An intricate state of affairs that befits the rich scaling features of a multifractal attractor. This dynamical organization is difficult to resolve from the consideration of a straightforward time evolution, i.e., starting from an arbitrary position x_0 within the attractor and recorded at every time t. In this case what is observed [14] are strongly fluctuating quantities that persist in time with a tangled pattern structure that presents memory retention. On the other hand, if specific initial positions with known location within the multifractal are chosen, and subsequent positions are observed only at preselected times, when the trajectories visit another region of choice, a well-defined q-exponential form for ξ_t emerges. The specific value of q and the associated Lyapunov spectrum λ_q can be clearly determined. For each case the value of q is given by the values of the trajectory scaling function σ at one of its discontinuities, while the corresponding spectrum λ_q reflects all starting positions in the multifractal region where the trajectories originate. We remind the reader that the results presented here are independent from the dynamics of approach to the attractor as we have not considered the time evolution of initial positions x_0 outside the attractor and leave this case for future attention.

Interestingly, the crossover from q statistics to BG statistics can be observed for control parameter values in the vicinity of the onset of chaos, $\mu \gtrsim \mu_\infty$, when the attractor consists of 2^n bands, n large. The Lyapunov coefficient λ_1 of the chaotic attractor decreases with $\Delta\mu = \mu - \mu_\infty$ as $\lambda_1 \propto 2^{-n} \sim \Delta\mu^\kappa$, $\kappa = \ln 2/\ln \delta(z)$, where δ is the second Feigenbaum constant [8]. The chaotic orbit consists of an interband periodic motion of period 2^n and an intraband chaotic motion. The expansion rate $\Sigma_{i=0}^{t-1} \ln|df_\mu(x_i)/dx_i|$ grows as $\ln t$ for $t < 2^n$ but as t for $t \gg 2^n$ [7,14]. This translates as Tsallis dynamics with $q \neq 1$ for $t < 2^n$ but BG dynamics with $q = 1$ for $t \gg 2^n$.

In summary, we have obtained further understanding about the nature of the dynamics at the onset of chaos in logistic maps. We exhibited links between original developments, such as Feigenbaum's σ function and Mori's q-phase transitions, with more recent advances, such as q-exponential sensitivity to initial conditions [5] and q-generalized identity between Lyapunov coefficients and rate of entropy change [6]. Chaotic orbits possess a time-irreversible property that stems from mixing in phase space and loss of memory, but orbits within critical attractors are nonmixing and have no loss of memory. Our results apply to many other unimodal

one-parameter families of maps. One example is the exponential function map $f(y)=1-\nu\exp(|y|^{-z})$ studied in Ref. [15] as the simple (monotonic) change of variable $|x|^z = \exp(|y|^{-z})$ indicates. Comparable results would be expected to hold for the two other routes to chaos [8], intermittency and quasiperidicity, in low-dimensional maps as these exhibit both q-phase transitions [7] and q sensitivity to initial conditions [4,19]. Clearly, our results establish a feasible numerical scheme to determine the family of values for the entropic index q associated to a critical multifractal attractor (here via the diameter function σ). Conversely, the computation of the sensitivity ξ_t at the onset of chaos offers an original means to evaluate Feigenbaum's trajectory scaling function σ or its equivalent for other critical attractors. Additionally and remarkably, the perturbation with noise of this attractor brings out the main features of glassy dynamics in thermal systems [20].

[1] C. Tsallis, J. Stat. Phys. **52**, 479 (1988).

[2] For recent reviews see, *Nonextensive Entropy—Interdisciplinary Applications*, edited by M. Gell-Mann and C. Tsallis (Oxford University Press, New York, 2004). See http://tsallis.cat.cbpf.br/biblio.htm for full bibliography.

[3] C. Tsallis, A. R. Plastino, and W.-M. Zheng, Chaos, Solitons Fractals **8**, 885 (1997).

[4] M. L. Lyra and C. Tsallis, Phys. Rev. Lett. **80**, 53 (1998).

[5] F. Baldovin and A. Robledo, Phys. Rev. E **66**, 045104(R) (2002).

[6] F. Baldovin and A. Robledo, Phys. Rev. E **69**, 045202(R) (2004).

[7] H. Mori, H. Hata, T. Horita, and T. Kobayashi, Prog. Theor. Phys. **99**, 1 (1989).

[8] H. G. Schuster, *Deterministic Chaos. An Introduction*, 2nd revised ed. (VCH Publishers, Weinheim, 1988).

[9] C. Beck and F. Schlogl, *Thermodynamics of Chaotic Systems* (Cambridge University Press, England, 1993).

[10] R. C. Hilborn, *Chaos and Nonlinear Dynamics*, 2nd revised ed. (Oxford University Press, New York, 2000).

[11] M. J. Feigenbaum, Commun. Math. Phys. **77**, 65 (1980); Physica D **7**, 16 (1983).

[12] P. Grassberger and M. Scheunert, J. Stat. Phys. **26**, 697 (1981).

[13] G. Anania and A. Politi, Europhys. Lett. **7**, 119 (1988). This work headed the determination of the spectrum of anomalous Lyapunov coefficients at the onset of chaos in the logistic map.

[14] H. Hata, T. Horita, and H. Mori, Prog. Theor. Phys. **82**, 897 (1989).

[15] G. F. J. Añaños and C. Tsallis, Phys. Rev. Lett. **93**, 020601 (2004).

[16] This is not a generalized Pesin identity that would involve a generalized Kolmogorov–Sinai entropy. We discuss this issue in a subsequent Section.

[17] E. Mayoral and A. Robledo, Physica A **340**, 219 (2004).

[18] V. Latora and M. Baranger, Phys. Rev. Lett. **82**, 520 (1999).

[19] F. Baldovin and A. Robledo, Europhys. Lett. **60**, 518 (2002).

[20] A. Robledo, Phys. Lett. A **328**, 467 (2004); F. Baldovin and A. Robledo, e-print cond-mat/0504033.